EUMETSAT
OSI SAF
OCEAN AND SEA ICE

Algorithm Theoretical Basis Document for the OSI SAF wind products

All scatterometer wind products in the ranges OSI-100 to OSI-113 and OSI-150 to OSI-159

Version: 1.7

Date: 24/10/2018

Ocean and Sea Ice SAF

Royal Netherlands
Meteorological Institute
*Ministry of Infrastructure
and Water Management*

Document Change record

Document version	Software version	Date	Author	Change description
1.0		Aug 2012	AV	Initial version
1.1		Feb 2014	AV	Changes resulting from SeaWinds reprocessing RR and PCR
1.2		Feb 2015	AV	Editorial changes for RapidScat
1.3		Jun 2016	AV	Editorial changes for OSCAT reprocessing RR and PCR, included review comments
1.4		Feb 2017	AV	Changes resulting from ERS reprocessing DRR
1.5		Feb 2017	AV	Comments from ScatSat PCR included
1.6		May 2018	AV	Implementation of CMOD7 for ASCAT and stress-equivalent model winds
1.7		Oct 2018	AV	Version for Requirement Review and Product Consolidation Review of wind data records

Table of contents

1. Introduction

The EUMETSAT Ocean and Sea Ice Satellite Application Facility (OSI SAF) produces a range of air-sea interface products, namely: wind, sea ice characteristics, Sea Surface Temperatures (SST) and radiative fluxes, Surface Solar Irradiance (SSI) and Downward Long wave Irradiance (DLI).

KNMI is involved in the OSI SAF as the centre where the level 1 to level 2 scatterometer wind processing is carried out. This document is the Algorithm Theoretical Basis Document to the wind products. More general information on the OSI SAF project is available on the OSI SAF web site: http://osi-saf.eumetsat.int/. Information about the specific wind products and their status can be found on http://www.knmi.nl/scatterometer/.

The scatterometer is an instrument that provides information on the wind field near the ocean surface, and scatterometry is the knowledge of extracting this information from the instrument's output. Space-based scatterometry has become of great benefit to meteorology and climate in the past years, see e.g. [1], [2].

KNMI has a long experience in scatterometer processing and is developing generic software for this purpose. Processing systems have been developed for the ERS, NSCAT, SeaWinds, ASCAT, Oceansat-2/OSCAT, RapidScat, HY-2A/HSCAT and ScatSat-1/OSCAT scatterometers. Scatterometer processing software is developed in the OSI SAF and provided through the EUMETSAT Numerical Weather Prediction Satellite Application Facility (NWP SAF), and is used in the wind processing performed operationally in the OSI SAF. The algorithms developed for the various steps in the wind retrieval are shared between the processing software for the different instruments, but some details differ depending on instrument characteristics like antenna configuration and frequency band used. This document provides a general overview and also briefly describes the differences between the instruments. The wind processing software package for C-band scatterometers (ASCAT Wind Data Processor, AWDP for ERS and ASCAT) is described in [3] and the software package for Ku-band pencil beam scatterometers (Pencil Beam Wind Processor, PenWP for SeaWinds, RapidScat, OSCAT and HSCAT) is described in [4].

Web resources that may be consulted and which complement this ATBD are:

- KNMI scatterometer website;
- KNMI publications website;
- Training course on applications of satellite wind and wave products for marine forecasting, available in video or document forms;
- International Ocean Vector Winds Science Team meeting presentations;

Following the introduction, section 2 of this document presents an overview of the various scatterometer instrument concepts, section 3 provides the processing algorithms and section 4 gives a brief overview of the wind processing of the different products in near-real time.

Please note that this document is limited to a qualitative description of the algorithms, including strengths and weaknesses, but without presenting too many formulas. This is done to increase the readability. The algorithms are more detailed in the references given.

2. Scatterometer instrument concepts

The scatterometer is a non-nadir looking real aperture radar instrument. Wind vector information over the oceans can be empirically derived from it. Over the last decades, scatterometers on-board satellites have provided very valuable sea surface wind field information. In addition to the meteorological and oceanographic use of scatterometer winds, the scatterometer data are of interest in applications such as sea ice detection and land surface soil moisture determination. In terms of antenna geometry, the scatterometer systems can be classified as side-looking and rotating scatterometers. Space borne scatterometer instruments are always mounted on low Earth orbiting platforms, most of the time polar orbiters. As a consequence of this, a specific location on Earth will normally be re-visited twice a day at maximum.

Side-looking scatterometers consist of a set of static fan-beam antennas pointing to one or both sides of the satellite flight track. Examples of such instruments are the NASA Scatterometer (NSCAT) on-board ADEOS-1, the scatterometers on the European Remote Sensing Satellites ERS-1 and ERS-2 [6], and the Advanced SCATterometer (ASCAT) on-board Metop. An example of the illumination pattern of a side-looking scatterometer is shown in Figure 1. This pattern shows the coverage of ASCAT which has, contrary to ERS, two sets of antennas looking to either side of the satellite ground track. ERS only has one set of three antennas looking to the right side of the satellite track.
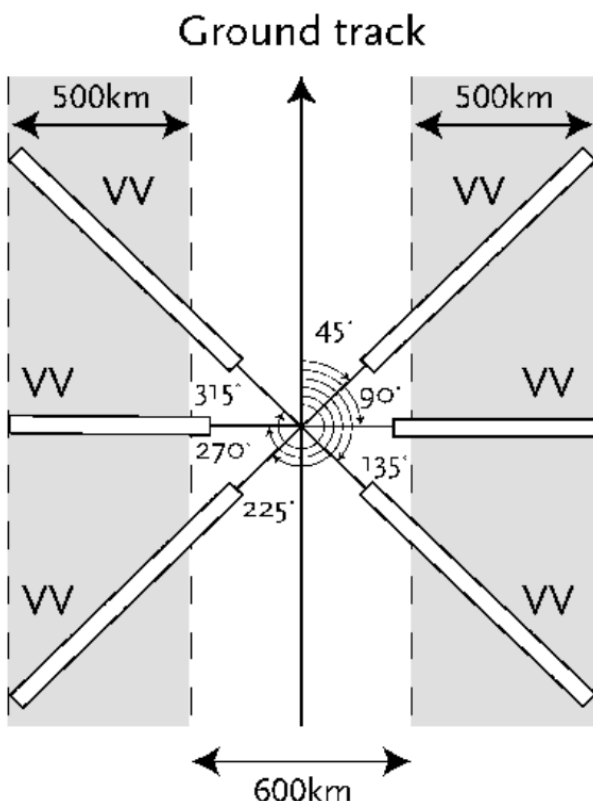
Figure 1: Earth surface coverage of the scans of the side-looking ASCAT scatterometer (source: [10]). Each location in the swaths is illuminated by the fore, the mid, and the aft beam as the satellite propagates towards the top of the page.

In contrast to side-looking scatterometers, the rotating scatterometers have a set of rotating antennas that sweep the Earth surface in a circular pattern as the satellite moves. The antennas can either be pencil (or spot) beams, as used for SeaWinds on-board QuikSCAT, OSCAT on-board Oceansat-2 and RapidScat on-board the International Space Station, or fan beams, as being built for the scatterometer on-board CFOSAT. See Figure 2 for the ground illumination pattern of SeaWinds or OSCAT. Due to the conical scanning, a swath location is generally viewed by each beam when looking forward (fore) and a second time when looking aft. As such, up to four measurement classes (called "view" here) emerge: horizontally polarised (HH) fore, HH aft, vertically polarised (VV) fore, and VV aft, in each Wind Vector Cell (WVC). The 1800-km-wide swath covers 90% of the ocean surface in 24 hours which represents a substantial improvement compared to the side-looking scatterometers like ERS and ASCAT.
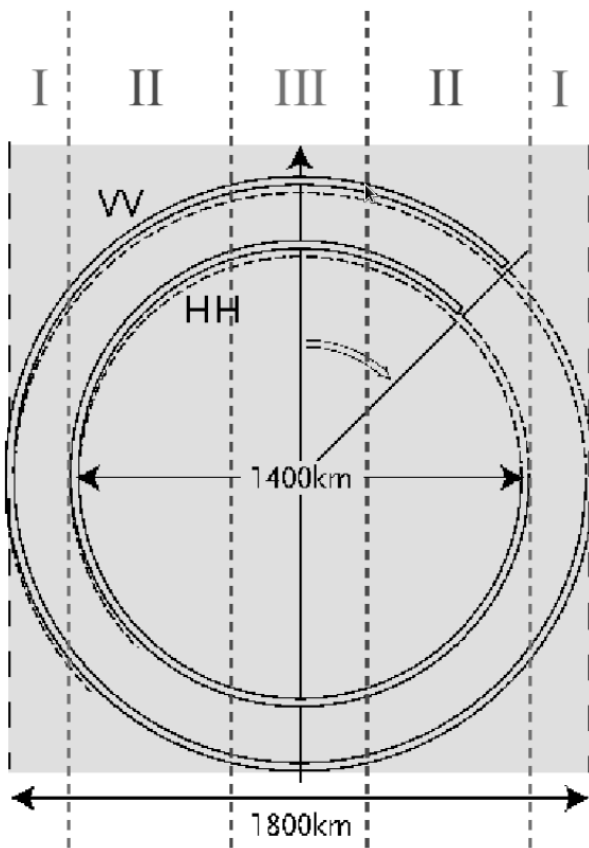
Figure 2: Earth surface coverage of the scans of the HH and VV pencil-beams of SeaWinds or OSCAT (source: [10]). As the satellite propagates towards the top of the page the swath (in grey) is illuminated, and three areas are discriminated:
I: Outer swath: only viewed once by the VV beam in the forward direction, and once in the aft direction (2 views), the azimuth view directions are very close and perpendicular to the satellite propagation direction;
II: Sweet (inner) swath: Viewed both by the VV and HH beam, both in fore and aft direction (4 views), the azimuth views are very diverse in direction;
III: Nadir (inner) swath: As II, but the azimuth view direction is close to the satellite propagation direction, or just opposite to it.

On the other hand, the wind retrieval from measurements of rotating scatterometers is more complex. In contrast with the side-looking scatterometers, the number of measurements and the beam azimuth angles vary with the sub-satellite cross-track location (see Figure 2). In the outer swath the situation is even more complicated since here only VV-polarised data are available. The wind retrieval skill will

therefore depend on the position in the swath, wind speed and wind direction. A detailed discussion of this matter is provided in [5]; pages 22-23. A detailed performance comparison study of different scatterometer concepts, based on simulation, is provided in [46].

Apart from the antenna configuration, scatterometers can also be distinguished with respect to the radar frequency band. The commonly used bands are C-band (~5.25 GHz or ~5 cm wavelength) and Ku-band (~13.5 GHz or ~2 cm wavelength). The smaller wavelength of Ku-band allows either a better spatial resolution for a given antenna size or a smaller antenna size for a given spatial resolution. On the other hand, the atmosphere is not transparent at Ku-band wavelengths and in particular rain is detrimental for wind computation. In fact, moderate and heavy rain cause bogus wind retrievals of 15-20 m/s wind speed [43] and rain contamination needs to be eliminated by a quality control step.

Land and sea ice contamination of a WVC will seriously disturb the wind retrieval. Land can be filtered out using a fixed land-sea mask. Discrimination of water and sea ice surfaces is generally best possible when both VV and HH polarisation measurements are available like for SeaWinds and OSCAT [7]. For ERS and ASCAT, which only have VV-polarised measurements available, the ice screening is more difficult, but still well possible [8]. In addition, prior wind and Sea Surface Temperature information can be used to prevent erratic winds over sea ice surfaces.

3. Algorithms

Scatterometry was developed heuristically. It was found experimentally that the sensitivity to wind speed and direction well describes the changes in backscatter over the ocean at moderate incidence angles due to changes in surface roughness. This is depicted in Figure 3 [9]. In return, backscatter measurements can be used to determine the wind speed and wind direction in a WVC.

A schematic illustration of the processing is given in figure 4. After defining the wind output and motivating the Geophysical Model Function that is used, the algorithms developed at KNMI are described.
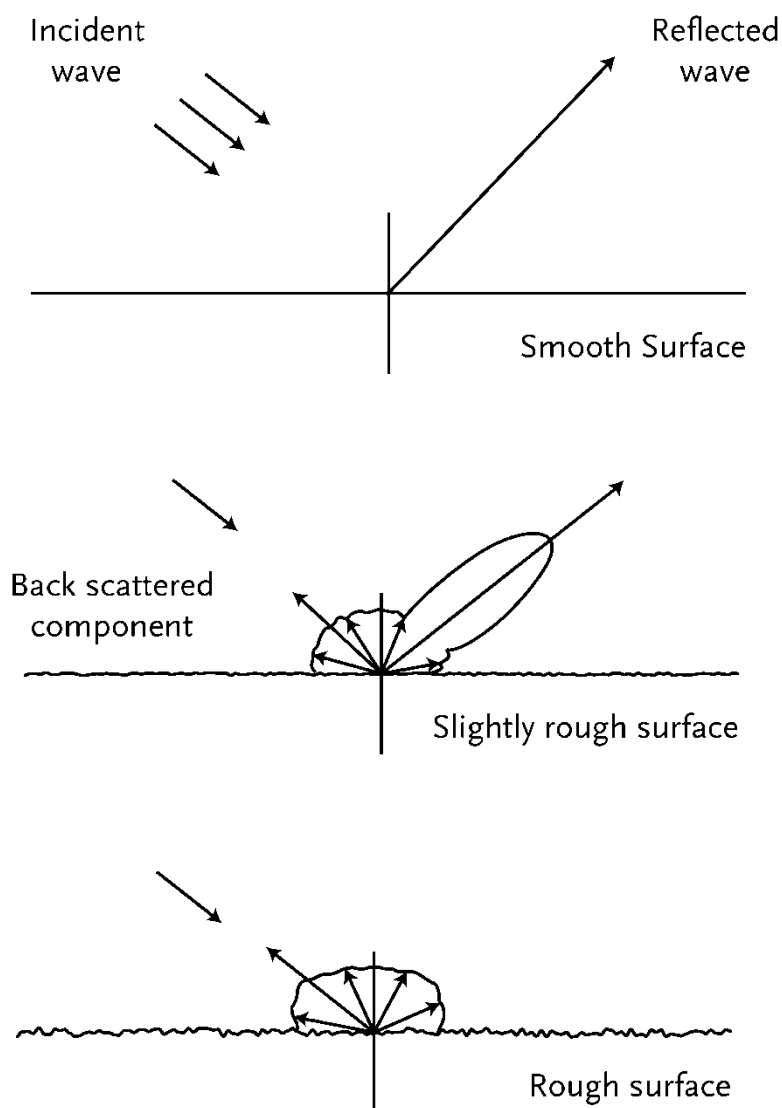
Figure 3: Schematic representation of microwave scattering and reflection at a smooth (top), rough (middle) and very rough (bottom) ocean surface. As the roughness increases more microwave power is returned towards the direction of the microwave source.

3.1. Wind defintion

A scatterometer measurement relates to the ocean surface roughness (see Figure 3), while the scatterometer product is represented by the stress-equivalent (SE) wind at 10 meter height over a WVC. The stress-equivalent wind transforms the sea surface roughness measurements to 10 m height in a unique way and independent of atmospheric stratification [24]. Moreover, SE winds are straightforward to compute at most buoy locations and from NWP model output for validation and comparison.

For NWP model winds, the conversion from real 10m winds to SE winds goes in two steps: firstly equivalent neutral (EN) winds are computed from real winds, sea surface temperature, air temperature, Charnock parameter and specific humidity, using a stand-alone implementation of the ECMWF model surface layer physics [25]. Note that this step is not needed for recent ECMWF data from the operational model and ERA5 re-analysis, since in these datasets the equivalent neutral winds are already available directly. The previous ERA-Interim re-analysis only provided real winds. The equivalent neutral winds subsequently are converted to stress-equivalent winds (U10S) by multiplying by a correction factor of $\sqrt{(\rho/<\rho>)}$, where ρ is the air density and $<\rho>$ is the average air density (1.225 kg/m^3).

The correction factor follows from the fact that the surface roughness as measured by the scatterometer is more closely correlated with surface stress τ than with the actual wind speed at 10 m. The surface stress τ is proportional to the air density and to the square of the equivalent neutral 10 m wind. In order to make the NWP winds equivalent to the scatterometer winds, we need to apply a correction, i.e. multiply by the square root of the normalised density. The air density is computed from the NWP model mean sea level pressure (*msl*), specific humidity (*q*) and air temperature (*T*) as $\rho = msl / (287.04 \times (1 + 0.6078 \times q) \times T)$ [26].

Note that in the conversion of real winds to SE winds, wind turning is neglected in the lowest 10 metres, so the direction of both winds will be the same. Typically, the largest difference is related to stability effects. Since the atmospheric boundary layer is on average weakly unstable, the SE wind will be on average slightly stronger than the real wind by approximately 0.1 to 0.2 m/s. Besides variations due to the local weather, there are typical seasonal variations. Generally, the SE wind speeds are more positively biased in colder regions and more negatively biased in warmer regions. More statistics are shown in [27].

It is important to realize that in the approach followed here the radar backscatter measurement σ^0 is related to the SE wind at 10 meter height above the ocean surface, simply because such wind measurements are widely available for validation as 10 m is a World Meteorological Organization (WMO) reference height. This means that any effect that relates to the mean wind vector at 10 meter height is incorporated in the backscatter-to-wind relationship. As such, the appearance of surface slicks, and the amplitude of gravity or longer ocean waves, depend to some degree on the strength of the wind and may, to the same degree, be fitted by a Geophysical Model Function, GMF ([10], Chapter I). Stoffelen ([10], Chapter IV) discusses a unique method to determine the accuracy of scatterometer, buoy, and NWP model winds by triple collocation.

```
┌─────────────────────────────────────┐
│   QC, NOC and Spatial Averaging      │
└─────────────────────────────────────┘
                  │
                  ▼
┌─────────────────────────────────────┐
│         NWP collocation              │
└─────────────────────────────────────┘
                  │
                  ▼
┌─────────────────────────────────────┐
│    Wind retrieval by GMF Inversion   │
└─────────────────────────────────────┘
                  │
                  ▼
┌─────────────────────────────────────┐
│         Quality Control              │
└─────────────────────────────────────┘
                  │
                  ▼
┌─────────────────────────────────────┐
│       Bayesian ice screening         │
└─────────────────────────────────────┘
                  │
                  ▼
┌─────────────────────────────────────┐
│    Fieldwise Ambiguity Removal       │
└─────────────────────────────────────┘
                  │
                  ▼
┌─────────────────────────────────────┐
│        Monitoring Module             │
└─────────────────────────────────────┘
```
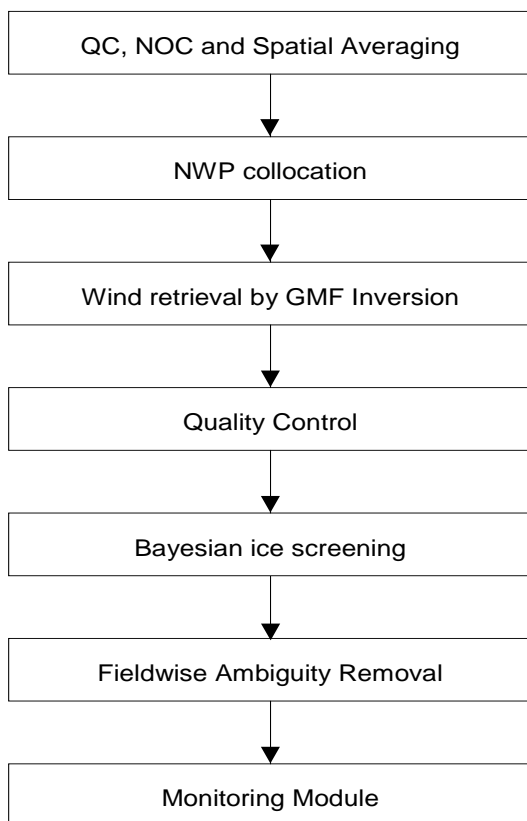
Figure 4: Overview of wind retrieval algorithm, QC denotes Quality Control and NOC denotes NWP Ocean Calibration.

At low wind speeds the wind direction and speed may vary considerably within the WVC. Locally, below a speed of roughly 2 m/s calm areas are present where little or no backscatter occurs, perhaps further extended in the presence of natural slicks that increase the water surface tension [11]. However, given the variability of the wind within a footprint area of 25 km it is, even in the case of zero mean vector wind, very unlikely that there are no patches with roughness in the footprint. As the mean vector wind increases, the probability of a calm patch will quickly decrease, and the mean microwave backscatter will increase. Also, natural slicks quickly disappear as the wind speed increases, and as such the occurrence of these is correlated to the amplitude of the mean vector wind over the footprint, as modelled by the GMF. Low scatterometer wind speeds are thus providing useful information [12], [13].

The wind variability varies on the globe. This implies for scatterometer measurements, being averaged over a large area, that the Probability Density Function (PDF) of contributing wind directions to a backscatter measurement varies over the globe as well. Wind direction variability acts to reduce the wind direction modulation of the GMF. For example, if wind blows from all directions in a WVC, then wind direction cannot be determined at all. On the other hand, steady winds tend to have higher wind direction GMF modulation than more nominal wind regimes. So, the anisotropy (azimuth direction dependence) of ocean radar backscatter is a function of local wind variability in the WVC (Figure 5).
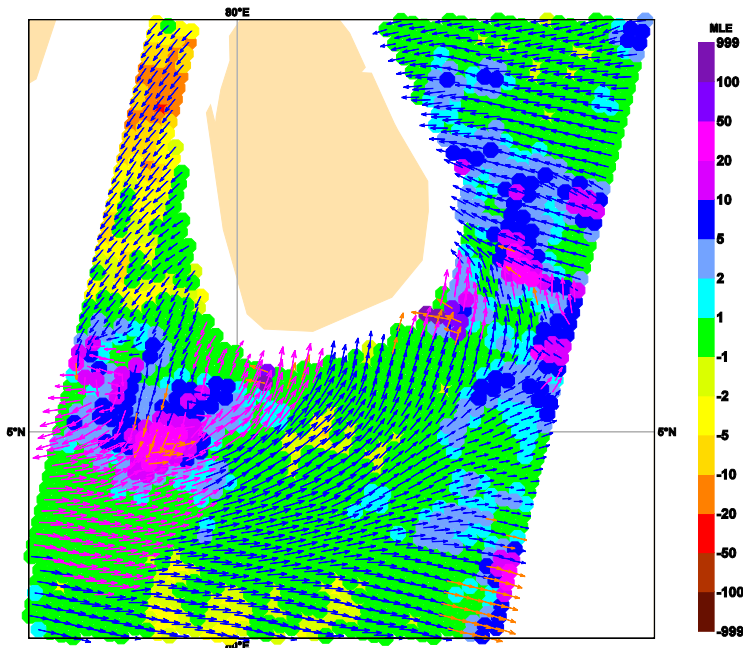
Figure 5: ASCAT wind (arrows) and wind variability (colours) at the ocean surface near Sri Lanka on 25 Nov 2011 3:45 UTC. The maximum winds just south of the island are 20 m/s; some of these wind arrows are coloured purple after flagging by 2DVAR, and some orange, after inversion Quality Control. The wind direction variability (which may be linked to the inversion residual or MLE, see section 3.6) is low to the northwest of the island (red colours; steady flow) and very high to the southwest and southeast (purple colours) due to severe convection that caused fatalities on this day.

At high wind speeds wave breaking will further intensify, causing air bubbles, foam and spray at the ocean surface, and a more and more complicated ocean topography. Although theoretically not obvious, it is empirically found that σ^0 keeps increasing for increasing wind speed from 25 m/s to 40 m/s, and that a useful wind direction dependency remains [14], albeit gradually weakening. HH (used for Ku-band scatterometers only) and VH polarization (planned for the second generation ASCAT, SCA on EPS-SG) measurements are more sensitive to extremely high winds than the nominal VV polarization [14].

3.2. Input screening

Backscatter input products contain flags to denote anomalous (instrument) conditions, which are obviously checked before wind retrieval and no retrieval is done in WVCs where these flags are raised. Examples of such flags are

- The ERS Missing Packet Counters (MPC) and ERS ESA Quality Control flag [15]. If the MPC value is below -18 or above 18, the beam information is rejected. The QC flags for beam arcing and frame checksum error are also evaluated.

- The ASCAT Sigma0 Usability Flag (must be at least 'usable')

- The OSCAT flags for 'Sigma0 is poor', 'Kp is poor', 'Invalid footprint' and 'Footprint contains saturated slice'.

- For SeaWinds and RapidScat: all bits in the SeaWinds Sigma0 Quality Flag, except the 'Negative' flag.

Additional tests concern the ranges of the input data, i.e., at least for backscatter values; noise estimates (K_p), azimuth and incidence angles, but also land occurrence and latitude and longitude position. Any data where the values are out of range are not used in the wind processing.

3.3. NWP Ocean Calibration

Mean ocean backscatter is quite variable following transient large-scale weather patterns. However, these weather patterns are well analysed in NWP and NWP information may be used to correct for these large-scale variations. Stoffelen [32] introduced NWP Ocean Calibration (NOC) and this method evolved to a powerful procedure to detect instrument anomalies and provide intercalibration of scatterometer systems, i.e., ERS and ASCAT or QuikSCAT and OSCAT. NOC is being employed for ERS [33] and ASCAT [34] in order to provide winds of constant quality. For OSCAT it is also considered [35], but not yet implemented since some issues remain that are not fully understood. The NOC procedure aims to find a representative mean backscatter value for each WVC view, independent of the weather, over a period of a year. NOC may be used for monitoring purposes as well over periods as short as a day or the entire mission [36].

3.4. Spatial representation

It is effective for radars to obtain individual backscatter measurements with a rather poor signal-to-noise ratio (SNR) of close to one or higher. In order to get an acceptable SNR on WVC level, multiple data acquisitions are spatially averaged over the WVC area. This results in a WVC level SNR of a few percent which is sufficient to obtain good quality winds. Each measurement field of view (FOV) has typical dimensions of 10 to 20 km, often smaller in one dimension than in the other, and the FOVs centred in a particular WVC will extend out of the WVC on all sides, leading to some WVC overlap [18]. It also leads to complications in scatterometer wind processing near land and sea ice boundaries and to the development of dedicated products, optimised in coastal regions [37].

The larger the WVC size chosen, the lower the noise in the averaged backscatter values, as more FOVs are integrated. Low noise and larger WVC sizes have advantages in NWP data assimilation, since NWP models do generally not resolve scales below 5-10 times their grid distance, see e.g. [38]. Lower resolution products are obtained by averaging available higher resolution backscatter products. On the other hand, in cases of extreme gradients (large signal), e.g., near polar lows or tropical hurricanes, shift meteorologists may appreciate high resolution winds, at the expense of some additional noise. The choice of spatial averaging approach allows addressing these preferences, after careful validation always ensuring that the resulting spatial representativeness of the data is adequate for the application intended.

In products optimised for coastal regions, for example, only FOVs over water are used to construct WVC backscatter values. This improves the wind coverage in coastal areas, but the WVC positions may be displaced away from the coast due to the exclusion of FOVs over land in the averaging. This leads to slight irregularities in the WVC spacing.

Note that the probability of occurrence of extremely high winds is substantially reduced by spatial averaging, since extreme winds are generally limited in spatial extent. Therefore, scatterometer winds

and NWP winds, lacking variability on the smallest scales, are expected to be associated with a narrower wind speed PDF than local buoy winds averaged over 1 or 10 minutes [39].

3.5. NWP collocation

NWP forecast wind data are necessary in the ambiguity removal step of the processing. Wind forecasts from the ECMWF global model are available twice a day (00 and 12 UTC analysis time, or 06 and 18 UTC analysis in case of the ERA5 re-analysis) with hourly forecast time steps of +3h, +4h, +5h and so on. The model wind data are quadratically interpolated with respect to time and bi-linearly interpolated with respect to location and put into the level 2 information part of each WVC. The ECMWF winds stored in the wind products are stress-equivalent winds [27] which have been computed from the equivalent neutral model winds.

It is important to note that scatterometer winds are being assimilated into the ECMWF model and therefore the wind field used for ambiguity removal (i.e., a forecast) is taken to be independent from the scatterometer observation. In near-real time processing the scatterometer measurement is received at approximately the same time at KNMI and ECMWF, and the scatterometer winds are produced at KNMI within a few minutes typically. Hence the observation cannot yet have been assimilated into the ECMWF model fields at the moment of processing at KNMI.

For scatterometer wind reprocessing, ERA-Interim or ERA5 data are used [40]; here observations are assimilated in the model up to 3 hours after the analysis time. Therefore, in the processing of those observations, only forecast winds starting from 3 hours after analysis time are used. In this way independence between the scatterometer and the ECMWF model winds used to guide the wind direction ambiguity removal, is guaranteed.

3.6. Wind retrieval

In scatterometer wind retrieval a Geophysical Model Function (GMF) is inverted. The radar backscatter of the ocean, as derived from the GMF, depends, besides on the wind vector w.r.t. the radar beam pointing, on radar wavelength (C-band or Ku-band) and vertical (VV) or horizontal (HH) polarization. The inversion step combines the backscatter measurements in a WVC to compute the WVC-mean wind vector. Subtle, but very relevant, differences exist in the GMFs and inversion steps of C-band fan-beam and Ku-band pencil-beam scatterometers.

3.6.1. Fan beam scatterometers

For the OSI SAF C-band scatterometer wind products (ERS and ASCAT), the CMOD7 GMF for calculating stress-equivalent neutral winds is used [22]. CMOD7 is based on CMOD5.n [23]. It is has been developed for intercalibrated ERS and ASCAT C-band scatterometer wind retrievals. As compared to CMOD5.n, CMOD7 better fits the sigma0 triplets at low wind speeds, and it provides more uniform wind speed probability functions across the satellite swath.

The GMF has two unknowns, namely wind speed and wind direction. So, if more than two backscatter measurements with Gaussian noise are available then these two unknowns may be estimated using a quadratic estimator as the objective function for determining the wind vector [16]. Based on Bayes' probability theorem, the Maximum Likelihood Estimator, *MLE,* is redefined by ([10], Chapter II):

$$MLE = \frac{1}{SD^2} \sum_{i=1}^{N} \left(z_{o,i} - z_{m,i} \right)^2$$

where $z_{o,i}$ are the backscatter measurements, $z_{m,i}$ are the simulated backscatter values corresponding to the measurements, $i \in (1,N)$, and SD is a measure of the measurement set noise standard deviation, related to both instrument noise and geophysical noise [17], [18]; $z = (\sigma^0)^{0.625}$ is a transformation that limits the wind direction sensitivity of the GMF to two harmonics. The wind direction sensitivity of the *MLE* function above is then approximately constant for the ERS and ASCAT fan-beam scatterometers and thus makes the inversion problem linear [17] and the *MLE* minima quadratic. The *MLE* value represents the probability of a trial wind vector (solution) being the 'true' wind, where higher *MLE*s correspond to lower probabilities and vice versa. Thus the wind inversion procedure consists of finding the minima in the *MLE*. The inversion of ERS and ASCAT measurement sets usually results in two well-defined local minima of the *MLE,* corresponding to two opposing wind vector solutions. The three independent measurements generally well sample the azimuth variation of the GMF and resolve the wind direction, albeit ambiguously.

3.6.2. Pencil beam scatterometers

For the OSI SAF Ku-band scatterometer wind products (like SeaWinds, OSCAT and RapidScat) the NSCAT-2 GMF for calculating SE winds was used in the past [19]. Portabella ([5]; appendix C) compared the QSCAT-1 [21] and NSCAT-2 Ku-band GMFs for SeaWinds wind retrieval. He found that the QSCAT-1 results in more wind solutions during wind retrieval, i.e., it is more ambiguous. In other words, for QSCAT-1 we generally find more minima when we inspect the *MLE* as a function of wind direction. Portabella verified that the additional minima are generally artificial and do not contribute to wind direction skill, i.e., act as a noise source. These additional local minima (noise) in the inversion potentially do result in local minima in ambiguity removal, even when using the so-called Multiple Solution Scheme (MSS), and thus in locally erroneous scatterometer wind field retrieval (see section 3.9).

A known problem of NSCAT-2 is that it overestimates wind speeds above 15 m/s, both when comparing to buoy winds and to NWP model winds. Hence, the NSCAT-2 GMF was changed for wind speeds above 15 m/s. The new GMF is called NSCAT-4. The NSCAT-4 GMF was derived from the NSCAT-2 GMF. Above 15 m/s, a linear scaling of the wind speed was applied. Subsequently, 0.2 m/s was added to all wind speeds.

$v_{NSCAT-4} = v_{NSCAT-2} + 0.2;$ $v <= 15$ m/s

$v_{NSCAT-4} = 2/3 * v_{NSCAT-2} + 5.2;$ $v > 15$ m/s

So, a backscatter value leading to an 8 m/s wind from NSCAT-2 corresponds to a 8.2 m/s NSCAT-4 wind and a 24 m/s wind from NSCAT-2 corresponds to a 21.2 m/s NSCAT-4 wind retrieval. The NSCAT-2 GMF lookup table was adapted in this way for all combinations of incidence and azimuth angles. This ensures that the fit in measurement space of the backscatter quadruplets to the GMF will not change. In [20] it was shown that NSCAT-4 provides a good fit of scatterometer wind speeds to both ECMWF and buoy winds. NSCAT-4 replaces NSCAT-2 for all Ku-band OSI SAF wind products.

In [17], Bayes' retrieval for the varying azimuth geometry of pencil-beam scatterometers is discussed and it is noted that such scatterometers are not sensitive to the wind vector for certain wind directions with a systematic variation by WVC. Therefore, the inversion procedure cannot be made linear and broad and skew *MLE* minima remain near these wind directions. Moreover, these wind directions "attract" local *MLE* minima and thus these local minima do not necessarily represent an optimal solution. The inherent broad and skew minima of pencil-beam scatterometers may be well represented in the wind vector solution space by the MSS that is used in the OSI SAF wind products [30]. In fact, for each wind direction the optimal speed is selected and its residual (*MLE*) is kept. The residuals are converted to probabilities, which are used in the ambiguity removal for all wind directions simultaneously, thus representing the full wind vector solution probability density function at each WVC.

3.7. Quality control

Since the scatterometer wind retrieval problem is over-determined, this opens up the possibility of quality control (QC) by checking the inversion residual. The inversion residual (*MLE*) is in theory inversely proportional to the log probability that a WVC is affected solely by a nominal, representative wind vector. Generally such probability is low, and the wind vector solution residual high, when rain affects the WVC, or when there is substantial wind or sea state variability within the cell [17], [18].

As such, Portabella and Stoffelen [28] found that the inversion residual is well capable of removing cases with extreme wind variability (at fronts or centres of lows), or with other geophysical variables affecting the radar backscatter, such as rain. QC is performed on the WVCs and rejection percentages vary between 3-7% for Ku-band and are below 1% for C-band systems. The KNMI QC procedure proves very effective, among others for screening rain in Ku-band scatterometers [43].

Steady flows show an increased harmonic dependence (anisotropy) of ocean radar backscatter and thus an elevated absolute *MLE* due to relatively poor correspondence with the GMF which has been derived for nominal wind conditions. Portabella et al. [44] found that the derived wind vectors are of good quality in such cases, but are degraded in cases of relatively isotropic ocean response. The latter are caused by (extreme) wind variability, rain splash [46] or perhaps confused sea states, which hamper the derivation of a representative wind vector. Therefore, a QC procedure has been implemented (for ERS and ASCAT) that only flags cases of increased isotropic response of the ocean backscatter [44].

3.8. Sea ice screening

Following the developments on Bayesian wind retrieval, [7] and [8] provide scatterometer sea ice GMF and retrieval procedures. In fact, combining both wind and sea ice retrievals, the probability of sea ice may be computed, which shows very good sensitivity of scatterometer systems to sea ice cover, including over the melt season where passive microwave techniques appear less sensitive [7]. NWP model sea surface temperature (SST) data are used to support the Bayesian sea ice discrimination. WVCs with a sea surface temperature above 5 °C are assumed to be always open water. The ice screening procedure may sometimes assign rainy WVCs erroneous as ice; using the extra SST criterion, WVCs in warmer areas will never be labelled as ice. Due to its rather high threshold value, the NWP SST ice screening will only be active in regions far away from the poles. The Bayesian sea ice screening is used both for C-band and Ku-band instrument data, except for ISS/RapidScat which does hardly observe any sea ice areas due to its lower orbit inclination. For RapidScat a simple discrimination based on ECMWF SST data is used.

3.9. Ambiguity Removal

Scatterometer winds have multiple ambiguities and there are up to four local minima after wind inversion in each WVC. These may be well-defined inversion minima, but also broad and skew minima (see section 3.3). The ambiguities are removed by applying constraints on the spatial characteristics of the output wind field, such as on rotation and divergence. The 2DVAR scheme closely resembles the 3D-var and 4D-var schemes applied in NWP data assimilation. Several ambiguity removal (AR) schemes were evaluated for ERS data [29]. In addition to the subjective comparison of AR schemes, a method for the objective comparison of AR performance among the different schemes was used. In [29] it is shown that this way of comparison is effective to evaluate the shortcomings of AR schemes, but also reveals a more general way forward to improve AR, which is followed up by adapting 2DVAR [41].

2DVAR uses a short-range NWP wind forecast valid at the time and location of the scatterometer measurements and subtracts it from the scatterometer wind solutions. The resulting ambiguous innovations and their probabilities are represented in the ambiguous scatterometer observation operator ([10], Chapter V). Vogelzang et al. [42] evaluate the general spatial covariance structure of these innovations and successfully apply the found NWP error covariance matrices in 2DVAR. Scatterometer observations appear generally spatially uncorrelated. The rotation and divergence structures in the specified NWP error covariances in 2DVAR have a clear effect on 2DVAR performance, while the quality of the prior forecast information appears less critical [41], [29].

To represent the variable inversion minima in the pencil-beam scatterometer processing, MSS is used. The probability density function of the wind solutions is represented by binning the full circle of possible wind directions into 144 equal sectors of 2.5° and for each wind direction an optimal wind speed with its corresponding probability is calculated in the wind retrieval step. Subsequently, the 144 solutions of each WVC are used in the AR to select the optimal solution.

3.10. Product monitoring

For global coverage products, it is possible to generate a product monitoring flag, based on a multi-step check. If in one product the number of WVC Quality Control rejections, the mean residual (*MLE*), or the wind speed bias with respect to the ECMWF NWP background is above certain threshold values, typically 5 times the RMS in the expected nominal values, then the monitoring event flag is raised since the product is suspicious. The threshold values are based on evaluation of the product statistics over a long period and maximise the probability of detection while minimising the false alarm rate [31].

In the case when the scatterometer product is not global but granular (like the ASCAT regional EARS products) and files containing only a few minutes of data are generated and disseminated in real-time, this mechanism raises problems if there are not enough data in one pass for a statistically valid check. The multi-step monitoring check is sensitive to noise which is larger when mean values are calculated over fewer WVCs. If, accordingly, the thresholds are set high, many bad products will pass the check. On the other hand, if the threshold values are set too low, too many false alarms will be raised. This problem is solved by evaluating not only the data of the last processed pass, but by evaluating an amount of most recent data equivalent to the amount of half an orbit, although possibly originating from several different read-outs. In case of instrument degradation or other problems, the monitoring event flag will be raised with some delay, inherent to the discontinuous nature of a regional data stream.

4. Wind processing

KNMI has wind processing chains in place for several instruments, currently for ASCAT and ScatSat-1 in near-real time. The near-real time processing of the scatterometer backscatter data to a wind product is done on KNMI's operational computing facilities. Reprocessing facilities exist or will be created for ERS, ASCAT, SeaWinds, RapidScat, OSCAT, and HY-2A.

The wind processing software is developed within the OSI SAF and consists of a generic part (called genscat) and a part that is specially designed to handle the data of a specific instrument. The genscat software consists of several modules devoted to e.g. reading and writing of BUFR and NetCDF data, collocation of scatterometer data with NWP fields, wind inversion and ambiguity removal. The instrument specific part of the software contains the main program control; it calls the different modules and routines in order to execute the processing steps as outlined in Figure 4.

Ancillary data from the ECMWF global model are present on a central location of the computing facilities. Scatterometer input swath data are normally received through the EUMETCast system. The granularity of the input data is different per product type: one input file containing from 3 minutes of data for ASCAT global products up to one orbit (90-100 minutes of data) for OSCAT and RapidScat. The granularity of the BUFR output data is the same as the granularity of the input data, for level 2 NetCDF the output data are always organised per orbit. Please see the corresponding Product User Manuals for more detailed information.

In the near-real time processing chains, a run control script is executed every few minutes and checks if any new data has arrived. If so, the new files are copied from the EUMETCast reception station location to a local directory, the NWP data valid at the time of the measurements is searched and the scatterometer data files are processed one by one. Each input file usually results in one output file containing wind data. Output files are sent to the KNMI FTP server, to the EUMETCast uplink station and to the GTS where appropriate.

In the reprocessing chains, long time series of wind products are created. Scatterometer and ECMWF input data are collected first from different archives and then the data processing and monitoring of the whole data set is controlled by a script. The reprocessing is not different from near-real time processing in terms of algorithm, it is different only in the way that archive data are used and that the latest version of the wind processing software is used, see the respective Product User Manuals for more information of the used software. Moreover, reanalysis ECMWF data are used (ERA-Interim in the OSI SAF CDOP2 phase or ERA5 in the CDOP3 phase) in the reprocessing chains rather than data from the operational ECMWF model.

5. References

[1] Bourassa M.A., A. Stoffelen, H. Bonekamp, P. Chang, D. B. Chelton, J. Courtney, R. Edson, J. Figa, Y. He, H. Hersbach, K. Hilburn, Z. Jelenak, K. A. Kelly, R. Knabb, T. Lee, E. J. Lindstrom, W. Timothy Liu, D. G. Long, W. Perrie, M. Portabella, M. Powell, E. Rodriguez, D. K. Smith, V. Swail, F. J. Wentz, 2009, "Remotely Sensed Winds and Wind Stresses for Marine Forecasting and Ocean Modeling", Published in the *Proceedings of OceanObs'09: Sustained Ocean Observations and Information for Society*, 2009, Community White Paper 10.5270/OceanObs09.cwp.08.

[2] Isaksen, L., and A. Stoffelen, ERS-Scatterometer Wind Data Impact on ECMWF's Tropical Cyclone Forecasts, *IEEE-Transactions on Geoscience and Remote Sensing*, 2000, 38 (4), 1885-1892

[3] Vogelzang, J., A. Verhoef, J. Verspeek, J. de Kloe and A. Stoffelen, AWDP User Manual and Reference Guide, version 3.0, NWPSAF-KN-UD-005, 2016

[4] Verhoef, A., J. Vogelzang, J. Verspeek and A. Stoffelen, PenWP User Manual and Reference Guide version 2.0, NWPSAF-KN-UD-009, 2015

[5] Portabella, M, thesis "Wind Field Retrieval from Satellite radar systems", 2002 (*)

[6] See https://earth.esa.int/web/sppa/mission-performance/esa-missions/ers-1/scatterometer/sensor-description and https://earth.esa.int/web/sppa/mission-performance/esa-missions/ers-2/scatterometer/sensor-description

[7] Belmonte Rivas, M. and A. Stoffelen, New Bayesian algorithm for sea ice detection with QuikSCAT, *IEEE Transactions on Geoscience and Remote Sensing*, 2011, 49, 6, 1894-1901, doi:10.1109/TGRS.2010.2101608.

[8] Belmonte, M., J. Verspeek, A. Verhoef and A. Stoffelen, Bayesian sea ice detection with the Advanced Scatterometer, *IEEE Transactions on Geoscience and Remote Sensing*, 2012, 50, 7, 2649-2657, doi:10.1109/TGRS.2011.2182356.

[9] Valenzuela, G. R., Theories for the interaction of electromagnetic and ocean waves - a review, *Bound. Layer Meteor.*, 1978, 13, 612-685

[10] Stoffelen, A., thesis "Scatterometry", 1998 (*)

[11] Donelan, M. A., and W. J. Pierson, Radar scattering and equilibrium ranges in wind-generated waves with application to scatterometry, *J. Geophys. Res.*, 1987, 92, 4971-5029

[12] Plant, W. J., Effects of wind variability on scatterometry at low wind speeds, *J. Geophys. Res.*, 2000, 105 (C7), 16,899–16,910, doi:10.1029/2000JC900043

[13] Shankaranarayanan, K., and M. A. Donelan, A probabilistic approach to scatterometer model function verification, *J. Geophys. Res.*, 2001, 106 (C9), 19,969–19,990, doi:10.1029/1999JC000189

[14] Fernandez, D. E., J. R. Carswell, S. Frasier, P. S. Chang, P. G. Black, and F. D. Marks, Dual-polarized C- and Ku-band ocean backscatter response to hurricane-force winds, *J. Geophys. Res.*, 2006, 111, C08013, doi:10.1029/2005JC003048

[15] Met Office, UK, ERS Products, WMO FM94 BUFR format, ER-IS-UKM-GS-0001, Version 4, Issue 2, 16 February 2001

[16] Pierson, W.J., Probabilities and statistics for backscatter estimates obtained by a scatterometer, *J. Geophys. Res.*, 1989, <u>94</u>, 9743-9759; correction in *J. Geophys. Res.*, 1990, <u>95</u>, 809

[17] Stoffelen, A. and M. Portabella, On Bayesian Scatterometer Wind Inversion, *IEEE Transactions on Geoscience and Remote Sensing*, 2006, <u>44</u>, 6, 1523-1533, doi:10.1109/TGRS.2005.862502.

[18] Portabella, M. and A. Stoffelen, Scatterometer backscatter uncertainty due to wind variability, *IEEE Transactions on Geoscience and Remote Sensing*, 2006, <u>44</u>, 11, 3356-3362, doi:10.1109/TGRS.2006.877952.

[19] Wentz, F.J., D.K. Smith, A model function for the ocean normalized radar cross section at 14 GHz derived from NSCAT observations, *J. Geophys. Res.*, 1999, <u>104</u> (C5), 11499-11514, doi:10.1029/98JC02148

[20] Verhoef, A., and A. Stoffelen, OSCAT winds validation report, OSI SAF report, SAF/OSI/CDOP2/KNMI/TEC/RP/196, 2012 (*)

[21] Jet Propulsion Laboratory, QuikSCAT Science Data Product User's Manual, version 3.0, JPL D-18053, 2006

[22] Stoffelen, A., J. Verspeek, J. Vogelzang and A. Verhoef, The CMOD7 Geophysical Model Function for ASCAT and ERS Wind Retrievals, *IEEE Journal of Selected Topics in Applied Earth O*, 2017, <u>10</u>, 5, 2123-2134, doi:10.1109/JSTARS.2017.2681806

[23] Verhoef, A., M. Portabella, A. Stoffelen and H. Hersbach, CMOD5.n - the CMOD5 GMF for neutral winds, OSI SAF report, SAF/OSI/CDOP/KNMI/TEC/TN/165, 2008 (*)

[24] Portabella, M. and A. Stoffelen, On Scatterometer Ocean Stress, *J. Atm. Oceanic Technol.*, 2009, <u>26</u>, 2, 368-382 (*)

[25] Hersbach, H., Assimilation of scatterometer data as equivalent-neutral wind, *ECMWF Technical Memorandum* 629, 2010

[26] ECMWF, Official IFS Documentation, Available through http://www.ecmwf.int/

[27] De Kloe, J., A. Stoffelen and A. Verhoef, Improved Use of Scatterometer Measurements by using Stress-Equivalent Reference Winds, *IEEE Journal of Selected Topics in Applied Earth O,* 2017, <u>10</u>, 5, 2340-2347, doi:10.1109/JSTARS.2017.2685242

[28] Portabella, M., Stoffelen, A., Quality Control and Wind Retrieval for SeaWinds, EUMETSAT fellowship report, 2002 (*)

[29] Stoffelen, A., S. de Haan, Y. Quilfen, and H. Schyberg, ERS Scatterometer Ambiguity Removal Comparison, OSI SAF report, 2000 (*)

[30] Portabella, M. and A. Stoffelen, A probabilistic approach for SeaWinds data assimilation, *Quart. J. Royal Meteor. Soc.*, 2004, <u>130</u>, 127-152

[31] de Vries, J., A. Stoffelen J. and Beysens, Ambiguity Removal and Product Monitoring for SeaWinds, NWP SAF report NWPSAF_KN_TR_001 (*)

[32] Stoffelen, A., A Simple Method for Calibration of a Scatterometer over the Ocean, *J. Atmos. Ocean. Technol.*, 1999, <u>16</u> (2), 275-282 (See [10], Appendix A (*))

[33] Stoffelen, A., J. Vogelzang and A. Verhoef, Verification of scatterometer winds, 10th International Winds Workshop, 20/2/2010-26/2/2010, M. Forsythe & J. Daniels (Ed), 2010, Tokyo, Japan, JMA, EUMETSAT (*)

[34] Verspeek, J., A. Stoffelen, A. Verhoef and M. Portabella, Improved ASCAT Wind Retrieval Using NWP Ocean Calibration, *IEEE Transactions on Geoscience and Remote Sensing*, 2012, 50, 7, 2488-2494, doi:10.1109/TGRS.2011.2180730 (*)

[35] Risheng, Y., A. Stoffelen, J. Verspeek and A. Verhoef, NWP Ocean Calibration of Ku-band scatterometers, IGARSS 2012 (IEEE), 22/7/2012-27/7/2012, 2012, Munich, Germany (*)

[36] Anderson, C., J. Figa, H. Bonekamp, J. Wilson, J. Verspeek, A. Stoffelen and M. Portabella, Validation of Backscatter Measurements from the Advanced Scatterometer on MetOp-A, *J. Atm. Oceanic Technol.*, 2012, 29, 77-88, doi:10.1175/JTECH-D-11-00020.1 (*)

[37] Verhoef, A., M. Portabella and A. Stoffelen, High-resolution ASCAT scatterometer winds near the coast, *IEEE Transactions on Geoscience and Remote Sensing*, 2012, 50, 7, 2481-2487, doi:10.1109/TGRS.2011.2175001 (*)

[38] Skamarock, W. C., Evaluating Mesoscale NWP Models Using Kinetic Energy Spectra, *Monthly Weather Review* 132, Dec. 2004, 3019-3032

[39] Vogelzang, J., A. Stoffelen, A. Verhoef and J. Figa-Saldaña, On the quality of high-resolution scatterometer winds, *J. of Geophysical Research*, 2011, 116, C10033, doi:10.1029/2010JC006640 (*)

[40] Berrisford, P. et al., The ERA-Interim archive, Version 2.0, ECMWF Publication, 2011

[41] Vogelzang, J., A. Stoffelen, A. Verhoef, J. de Vries and H. Bonekamp, Validation of two-dimensional variational ambiguity removal on SeaWinds scatterometer data, *J. Atm. Oceanic Technol.*, 2009, 7, 26, 1229-1245, doi:10.1175/2008JTECHA1232.1 (*).

[42] Vogelzang, J. and A. Stoffelen, NWP Model Error Structure Functions obtained from Scatterometer Winds, *IEEE Transactions on Geoscience and Remote Sensing*, 2012, 50, 7, 2525-2533, doi:10.1109/TGRS.2011.2168407 (*).

[43] Portabella, M. and A. Stoffelen, Rain Detection and Quality Control of SeaWinds, *J. Atm. Oceanic Technol.*, 2001, 18, 7, 1171-1183, doi:10.1175/1520-0426(2001)018<1171:RDAQCO>2.0.CO;2

[44] Portabella, M., A. Stoffelen, A. Verhoef and J. Verspeek, A new method for improving ASCAT wind quality control, *IEEE Geosci. Remote Sensing Letters*, 2012, 9, 4, 579-583, doi:10.1109/LGRS.2011.2175435 (*).

[45] Portabella, M., A. Stoffelen, W. Lin, A. Turiel, A. Verhoef, J. Verspeek and J. Ballabrera-Poy, Rain Effects on ASCAT-Retrieved Winds: Toward an Improved Quality Control, *IEEE Transactions on Geoscience and Remote Sensing*, 2012, 50, 7, 2495-2506, doi:10.1109/TGRS.2012.2185933 (*).

[46] Lin, C.C., M. Betto, M. Belmonte-Rivas, A. Stoffelen and J. de Kloe, EPS-SG Wind Scatterometer Concept Trade-offs and Wind Retrieval Performance Assessment, *IEEE Transactions on Geoscience and Remote Sensing*, 2012, 50, 7, 2458-2472, doi:10.1109/TGRS.2011.2180393 (*).

References marked with a (*) are available on http://www.knmi.nl/scatterometer/publications/.

6. Abbreviations and acronyms

2DVAR	Two-dimensional Variational Ambiguity Removal
AR	Ambiguity Removal
ASCAT	Advanced Scatterometer
AWDP	ASCAT Wind Data Processor
CDOP	Continuous Development and Operations Phases of the SAFs
EN	Equivalent Neutral
EPS-SG	Second Generation of the European Polar Satellites
ERS	European Remote-Sensing Satellite
EARS	EUMETSAT Advanced Retransmission Service
EUMETCast	EUMETSAT's Digital Video Broadcast Data Distribution System
EUMETSAT	European Organisation for the Exploitation of Meteorological Satellites
GMF	Geophysical Model Function
HH	Horizontal polarisation of sending and receiving radar antennas
HSCAT	Scatterometer on-board the Chinese HY-2A satellite
JPL	Jet Propulsion Laboratory (NASA)
KNMI	Royal Netherlands Meteorological Institute
MLE	Maximum Likelihood Estimator
MSS	Multiple Solution Scheme
NASA	National Aeronautics and Space Administration (USA)
NOAA	National Oceanic and Atmospheric Administration (USA)
NOC	NWP Ocean Calibration
NSCAT	NASA Scatterometer
NWP	Numerical Weather Prediction
OSCAT	Scatterometer on-board the Indian Oceansat-2 satellite
OSI SAF	Ocean and Sea Ice SAF
PenWP	Pencil Beam Wind Processor
PDF	Probability Density Function
QC	Quality Control
QuikSCAT	USA dedicated scatterometer mission
RapidScat	SeaWinds-like scatterometer on-board the International Space Station
SAF	Satellite Application Facility
SCA	Scatterometer on EPS-SG, the successor of ASCAT

SE	Stress Equivalent
SeaWinds	Scatterometer on-board QuikSCAT platform (USA)
SST	Sea Surface Temperature
u	West-to-east wind component
v	South-to-north wind component
VV	Vertical polarisation of sending and receiving radar antennas
WMO	World Meteorological Organization
WVC	Wind Vector Cell